



# Differential cross section predictions for PRad-II from dispersion theory

Yong-Hui Lin<sup>a,\*</sup>, Hans-Werner Hammer<sup>b,c</sup>, Ulf-G. Meißner<sup>a,d,e</sup>

<sup>a</sup> Helmholtz-Institut für Strahlen- und Kernphysik and Bethe Center for Theoretical Physics, Universität Bonn, D-53115 Bonn, Germany

<sup>b</sup> Technische Universität Darmstadt, Department of Physics, 64289 Darmstadt, Germany

<sup>c</sup> ExtreMe Matter Institute EMMI, GSI Helmholtzzentrum für Schwerionenforschung GmbH, 64291 Darmstadt, Germany

<sup>d</sup> Institute for Advanced Simulation, Institut für Kernphysik and Jülich Center for Hadron Physics, Forschungszentrum Jülich, D-52425 Jülich, Germany

<sup>e</sup> Tbilisi State University, 0186 Tbilisi, Georgia



## ARTICLE INFO

### Article history:

Received 29 November 2021

Accepted 17 February 2022

Available online 21 February 2022

Editor: A. Ringwald

## ABSTRACT

We predict the differential cross sections for  $e^-p$  and  $e^+p$  elastic scattering in the PRad-II energy region. The prediction is based on form factors obtained in our previous high-precision analysis of space- and time-like data from dispersion theory and different sets of two-photon exchange corrections. We investigate the sensitivity of the cross sections to two-photon exchange effects and find that the differences between model calculations and phenomenological extractions of two-photon corrections can not be resolved if the uncertainty in the form factors is taken into account.

© 2022 The Author(s). Published by Elsevier B.V. This is an open access article under the CC BY license (<http://creativecommons.org/licenses/by/4.0/>). Funded by SCOAP<sup>3</sup>.

## 1. Introduction

The nucleon form factors (NFFs) are defined as the coefficients of the two independent Dirac structures in the general form of the electromagnetic  $\gamma NN$  vertex function. The electric and magnetic Sachs form factors  $G_E$  and  $G_M$  are scalar functions of the four-momentum transfer  $Q^2$  of the photon and encapsulate the structure of the nucleon as seen by an electromagnetic probe. The first experimental measurement of NFFs was carried out by Hofstadter and collaborators at the Stanford High Energy Physics Laboratory in 1953 [1,2]. The understanding of electromagnetic nucleon structure was further refined with the advent of continuous beam electron facilities such as MAMI and Jefferson Lab in the 1980's. At low momentum transfers this line of investigations appeared to be complete at the end of the last century. However, a renaissance of the NFF studies in the 2000's was triggered by the emergence of the so-called proton radius puzzle, based on the precise measurement of the Lamb shift in muonic hydrogen, which led to the determination of the proton charge radius at an unprecedented precision,  $r_E^p = 0.8484(67)$  fm [3,4]. This value differed by  $5\sigma$  from the CODATA value at that time [5], which was based on electron scattering experiments and measurements of the Lamb shift in ordinary hydrogen. For recent reviews of the NFFs see, e.g., Refs. [6–8].

The charge radius of the proton is defined as the derivative of its electric form factor at zero momenta transfer, that is,  $\langle (r_E^p)^2 \rangle = -6dG_E^p/dQ^2(Q^2=0)$  [9]. This makes the first-principle calculation from Quantum Chromodynamics (QCD) very difficult due to the non-perturbative nature of QCD in the low-energy region. In lattice QCD, disconnected contributions to the isoscalar form factors have proven to be a persistent challenge. See, e.g., Ref. [10] for the state of the art of lattice QCD calculations. A dispersion theoretical approach was proposed to analyze the electromagnetic structure of the nucleon at the very beginning of experimental investigations [11–13], which includes all constraints from unitarity, analyticity and crossing symmetry. It was further developed in subsequent works [14,15] to include new experimental data and to be consistent with the strictures from perturbative QCD at very large momentum transfer [16]. An important recent development is the improved determination of the isovector spectral functions from the two-pion continuum [17], based on an analysis of the Roy-Steiner equations for pion-nucleon scattering [18]. A comprehensive review of the state of the art of dispersive analyses of the nucleon electromagnetic form factors is given in Ref. [19]. The proton radius obtained in such analyses agrees well with the “small” proton charge radius from muonic hydrogen and is quite robust. It has remained around the value  $\langle (r_E^p)^2 \rangle^{1/2} \simeq 0.84$  fm since Höhler and collaborators pioneering work in the 1970's [13] despite many new experimental measurements and thus predates the muonic hydrogen experiments, see e.g. Ref. [20] for a discussion of the history.

Very recently, a comprehensive analysis of all latest  $e^-p$  elastic scattering (space-like,  $Q^2 > 0$ ) and  $e^+e^- \rightarrow N\bar{N}$  annihilation (time-like,  $Q^2 < 0$ ) data was performed in Ref. [21] within the

\* Corresponding author.

E-mail addresses: [yonghui@hiskp.uni-bonn.de](mailto:yonghui@hiskp.uni-bonn.de) (Y.-H. Lin), [hans-werner.hammer@physik.tu-darmstadt.de](mailto:hans-werner.hammer@physik.tu-darmstadt.de) (H.-W. Hammer), [meissner@hiskp.uni-bonn.de](mailto:meissner@hiskp.uni-bonn.de) (U.-G. Meißner).

dispersion theoretical framework. In the space-like region, the momentum transfer range  $Q^2 = 0.000215\text{--}0.977 (\text{GeV}/c)^2$  is covered, which consists mainly of the cross section data from MAMI-C [22] and PRad [23]. In the time-like region it includes data in the region  $|Q^2| = 3.52\text{--}20.25 (\text{GeV}/c)^2$  that is mainly composed of the effective form factor data from BESIII [24,25] and BaBar [26].<sup>1</sup> A set of nucleon form factors that describes all existing experimental data both in the space- and time-like regions over the full range of momentum transfers was obtained. In addition, the extracted form factors are also consistent with the measurements of Lamb shift and hyperfine splittings in muonic hydrogen as discussed in [21]. Starting from this set of NFFs, one can predict the electromagnetic properties of nuclei and experimental cross sections that will be measured in the future.

Recently, two upgraded projects based on the PRad setup for the  $e^-p$  and  $e^+p$  elastic scattering were proposed in Refs. [27] and [28], respectively. The former is also called PRad-II. In this work, we calculate the differential cross sections for the  $e^-p$  and  $e^+p$  elastic scattering in the energy region where the PRad-II experiment will run based on the high-precision nucleon form factors obtained in Ref. [21]. The results serve as predictions for the upcoming PRad-II and  $e^+p$  scattering measurements.

## 2. Formalism

Here, we briefly summarize the underlying formalism, which is detailed in Ref. [15,29,19]. When working with the one-photon-exchange assumption, the differential cross section for  $e^-p$  scattering can be expressed through the Sachs form factors  $G_E$  and  $G_M$  as

$$\frac{d\sigma_{1\gamma}}{d\Omega} = \left(\frac{d\sigma}{d\Omega}\right)_{\text{Mott}} \frac{\tau}{\epsilon(1+\tau)} \left[ G_M^2(Q^2) + \frac{\epsilon}{\tau} G_E^2(Q^2) \right], \quad (1)$$

where  $\epsilon = [1 + 2(1+\tau)\tan^2(\theta/2)]^{-1}$  is the virtual photon polarization,  $\theta$  is the electron scattering angle in the laboratory frame,  $\tau = Q^2/4m_N^2$ , with  $Q^2 > 0$  the four-momentum transfer squared and  $m_N$  the nucleon mass. It is well known as the Rosenbluth formula. Moreover,  $(d\sigma/d\Omega)_{\text{Mott}}$  is the Mott cross section, which describes scattering off a point-like spin-1/2 particle. To be compatible with the experimental data, the theoretical calculation must go beyond the one-photon approximation and in principle should consider all higher order corrections which are not negligible at the accuracy of experiments. However, these corrections, mainly composed of the radiative corrections, have usually been subtracted when the experiments present their measurements. The majority of them are estimated with the model-independent formalism which been widely investigated in the literature [30–35]. In contrast, the two-photon-exchange (TPE) contribution [36], which contains a relatively large uncertainty due to its model-dependent nature, is treated differently in various experiments. For example, MAMI-C uses a combination of the soft-photon limit [37,31] and a two-parameter empirical parametrization to account for the TPE correction, while a dispersive formalism [38,39] is used in the PRad experiment. In the present work, the differential cross sections of  $e^\pm p$  scattering are calculated in the one-photon approximation Eq. (1) and TPE corrections are applied. The sensitivity of the cross section to different sets of TPE corrections is investigated.

The leading TPE contribution is given by the interference between the one-photon and two-photon exchange amplitudes,  $\mathcal{M}_{1\gamma}$  and  $\mathcal{M}_{2\gamma}$ , respectively. It can be accounted for by including a modifying factor in Eq. (1). In the case of  $e^-p$  scattering, the cross section including two-photon corrections can be written as

$$\begin{aligned} \left(\frac{d\sigma_{\text{corr}}}{d\Omega}\right)_{e^-p} &= \frac{d\sigma_{1\gamma}}{d\Omega} (1 + \delta_{2\gamma}), \\ \delta_{2\gamma} &= \frac{2\text{Re}(\mathcal{M}_{1\gamma}^* \mathcal{M}_{2\gamma})}{|\mathcal{M}_{1\gamma}|^2} (1 + \mathcal{O}(\alpha)). \end{aligned} \quad (2)$$

For the two-photon exchange amplitude  $\mathcal{M}_{2\gamma}$ , we adopt the calculations of Refs. [29,19]. The box and crossed box diagrams are evaluated in the framework of a hadronic model with both the nucleon and  $\Delta$ -resonance contributions included [29]. The update made in the present work refers to the one-photon amplitude  $\mathcal{M}_{1\gamma}$  where the latest dispersive NFFs from Ref. [21] are used. This set of TPE corrections is representative for such model calculations and other calculations give consistent results [36].

The energy parameters of PRad-II are taken from the proposal [27]: three incident electron beams with energy  $E_e = 0.7, 1.4, 2.1 \text{ GeV}$  at very small scattering angles  $\theta_e$  from  $0.5^\circ$  to  $7^\circ$ , corresponding to  $Q^2 = 4 \times 10^{-5}$  to  $6 \times 10^{-2} (\text{GeV}/c)^2$ . This new experiment is designed to achieve a factor of 3.8 reduction in the overall experimental uncertainties of the extracted proton radius compared to PRad. With such an improvement of precision, it is expected to address possible systematic difference between the radius from  $e^-p$  and  $\mu H$  measurements. The proposed  $e^+p$  scattering would use the same setup as the PRad-II experiment [28]. The cross section of  $e^+p$  scattering is exactly same as that of  $e^-p$ , except that the factor  $(1 + \delta_{2\gamma})$  in Eq. (2) must be changed to  $(1 - \delta_{2\gamma})$ .

## 3. Results

Now let us move to the differential cross sections. For easier comparison with PRad [23] and the PRad-II proposal [27], we calculate the reduced cross section  $\sigma_{\text{reduced}}$  defined as

$$\begin{aligned} \sigma_{\text{reduced}} &\equiv \left(\frac{d\sigma}{d\Omega}\right)_{ep} \times \left[\left(\frac{d\sigma}{d\Omega}\right)_{\text{Mott}} \frac{E'/E}{1+\tau}\right]^{-1} \\ &= \frac{E}{\epsilon E'} \left[ \tau G_M^2(Q^2) + \epsilon G_E^2(Q^2) \right], \end{aligned} \quad (3)$$

where  $E$  and  $E'$  are the incoming and outgoing electron energies in the laboratory frame. In Fig. 1, we show  $\sigma_{\text{reduced}}$  in the energy regions probed by PRad and PRad-II. Although there is a large overlap in the energy region measured in the PRad-II and PRad experiments evident in Fig. 1, the uncertainty reduction and lower  $Q^2$  extension proposed in PRad-II are extremely important for the extraction of the proton radius.

The difference in the reduced cross sections for  $e^+p$  and  $e^-p$  scattering for the 0.7, 1.4, and 2.1 GeV energy beams is shown in Fig. 2. It is only due to TPE effects and thus rather small. Furthermore, we investigate the effect of TPE corrections on the predicted differential cross sections in detail. Two different schemes for TPE corrections, the box-graph model from Refs. [29,19], which is representative for hadronic model calculations of TPE, and the phenomenological parametrization from Bernauer et al. [22] are compared in Fig. 3 as a function of the scattering angle  $\theta$ . The cross sections are normalized to ones calculated using the dipole Sachs FFs to make the deviation among various TPE corrections transparent. Within the uncertainties of the NFFs, the cross sections with the box-graph model TPE are in agreement with those calculated by the parametrization obtained in Ref. [22].<sup>2</sup> The largest deviations occur for larger angles corresponding to the higher  $Q^2$ -range as expected. It turns out that the uncertainty emerging from

<sup>1</sup> Only the data basis covering the main energy range are listed here. The full data basis used in that comprehensive analysis can be found in Ref. [21].

<sup>2</sup> In principle, the uncertainties in the NFFs should also enter the box-graph TPE calculation as discussed in Sec. 2. However, the magnitude of the uncertainty in the TPE correction is a second order effect and thus quite small.

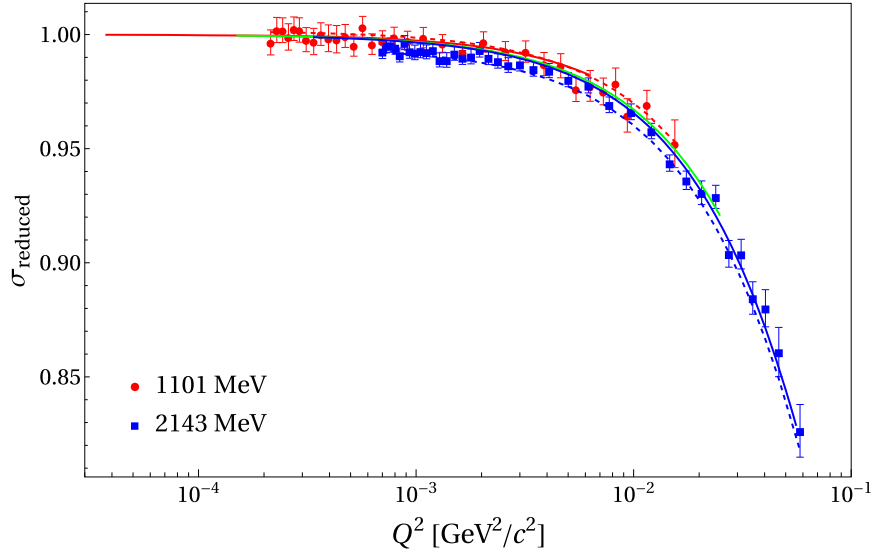


**Fig. 1.** Reduced cross section  $\sigma_{\text{reduced}}$  in the energies regions probed by PRad and PRad-II. The PRad data [23] is shown for comparison by the red solid circles (1.1 GeV data) and blue solid squares (2.2 GeV data). The red and blue dashed lines show our corresponding results for PRad. The red, green and blue solid lines are our predictions for the 0.7, 1.4 and 2.1 GeV energy beams of PRad-II, respectively.

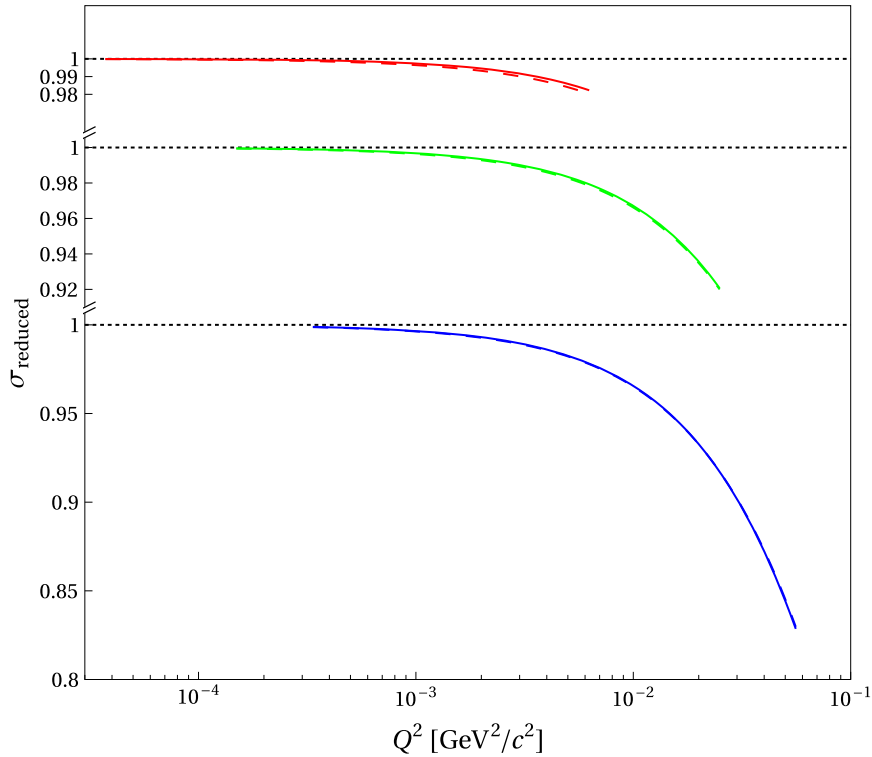


**Fig. 2.** Reduced cross section  $\sigma_{\text{reduced}}$  for the PRad-II (solid) and positron-proton scattering (dashed) experiments. The red, green and blue color represent the results for the 0.7, 1.4 and 2.1 GeV energy beams.

the model-dependent TPE corrections becomes a secondary effect when it is compared with the NFF uncertainties in the PRad-II energy region. The high-precision data from PRad-II thus will provide strong constraints on the nucleon form factors and help us improve the precision of our dispersive NFFs in Ref. [21].

Another interesting issue that the positron-proton scattering experiment would address is the ratio of cross sections for  $e^+p$  and  $e^-p$  scattering. It will give direct access to the TPE corrections. This can be seen clearly from Fig. 3, where the sign of the deviation between two different TPE calculations is opposite for the  $e^-p$  and

$e^+p$  scattering processes. This implies a large effect in the ratio of cross sections. We will come back to this issue in a future study (see also Ref. [36] for a recent review).

#### 4. Summary

In this paper, we present a prediction for the differential cross sections for the upcoming PRad-II and positron-proton scattering experiments based on the dispersive nucleon form factors obtained in Ref. [21]. Moreover, the effect of two-photon-exchange correc-

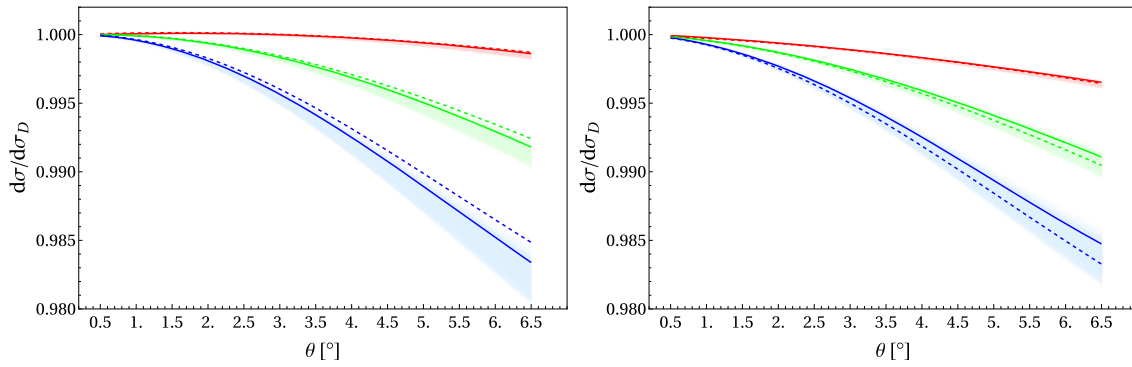


**Fig. 3.** Differential cross sections normalized to the cross section for dipole Sachs FFs for the PRad-II (left panel) and  $e^+p$  scattering (right panel) experiments. The red, green, and blue solid lines are the results with the box-graph TPE for the 0.7, 1.4 and 2.1 GeV energy beams, respectively. The corresponding dashed lines show the results with the phenomenological TPE from Bernauer et al. [22]. The uncertainties from the NFFs are presented as the shaded bands.

tions is also discussed. We find that the uncertainty caused by the model-dependent nature of TPE corrections is a secondary contribution when compared to the uncertainties in the NFFs errors for the PRad-II setup. The high-precision PRad-II data will provide strong constraints on the nucleon form factors and improve our knowledge of the electromagnetic structure of the nucleon. Finally, the theoretical uncertainties of the two-photon-exchange corrections need to be investigated further together with the positron-proton scattering data that will be available in the near future.

### Declaration of competing interest

The authors declare that they have no known competing financial interests or personal relationships that could have appeared to influence the work reported in this paper.

### Acknowledgements

This work of UGM and YHL is supported in part by the DFG (Project number 196253076 - TRR 110) and the NSFC (Grant No. 11621131001) through the funds provided to the Sino-German CRC 110 “Symmetries and the Emergence of Structure in QCD”, by the Chinese Academy of Sciences (CAS) through a President’s International Fellowship Initiative (PIFI) (Grant No. 2018DM0034), by the VolkswagenStiftung (Grant No. 93562), and by the EU Horizon 2020 research and innovation programme, STRONG-2020 project under grant agreement No 824093. HWH was supported by the Deutsche Forschungsgemeinschaft (DFG, German Research Foundation) – Projektnummer 279384907 – CRC 1245 and by the German Federal Ministry of Education and Research (BMBF) (Grant no. 05P21RDFNB). Further, this project has received funding from the European Research Council (ERC) under the European Union’s Horizon 2020 research and innovation programme (grant agreement No. 101018170).

### References

- [1] R. Hofstadter, H.R. Fechter, J.A. McIntyre, *Phys. Rev.* **91** (1953) 422.
- [2] R. Hofstadter, *Rev. Mod. Phys.* **28** (1956) 214.
- [3] R. Pohl, et al., *Nature* **466** (2010) 213.
- [4] A. Antognini, et al., *Science* **339** (2013) 417.
- [5] P.J. Mohr, B.N. Taylor, D.B. Newell, *J. Phys. Chem. Ref. Data* **37** (2008) 1187.
- [6] A. Denig, G. Salme, *Prog. Part. Nucl. Phys.* **68** (2013) 113, arXiv:1210.4689 [hep-ex].
- [7] S. Pacetti, R. Baldini Ferrolri, E. Tomasi-Gustafsson, *Phys. Rep.* **550–551** (2015) 1.
- [8] V. Punjabi, C.F. Perdrisat, M.K. Jones, E.J. Brash, C.E. Carlson, *Eur. Phys. J. A* **51** (2015) 79, arXiv:1503.01452 [nucl-ex].

- [9] G.A. Miller, *Phys. Rev. C* **99** (2019) 035202, arXiv:1812.02714 [nucl-th].
- [10] D. Djukanovic, T. Harris, G. von Hippel, P.M. Junnarkar, H.B. Meyer, D. Mohler, K. Ottnad, T. Schulz, J. Wilhelm, H. Wittig, *Phys. Rev. D* **103** (2021) 094522, arXiv:2102.07460 [hep-lat].
- [11] G.F. Chew, R. Karplus, S. Gasiorowicz, F. Zachariasen, *Phys. Rev.* **110** (1958) 265.
- [12] P. Federbush, M.L. Goldberger, S.B. Treiman, *Phys. Rev.* **112** (1958) 642.
- [13] G. Höhler, E. Pietarinen, I. Sabba Stefanescu, F. Borkowski, G.G. Simon, V.H. Walther, R.D. Wendling, *Nucl. Phys. B* **114** (1976) 505.
- [14] P. Mergell, U.-G. Meißner, D. Drechsel, *Nucl. Phys. A* **596** (367) (1996), arXiv:hep-ph/9506375.
- [15] M.A. Belushkin, H.-W. Hammer, U.-G. Meißner, *Phys. Rev. C* **75** (2007) 035202, arXiv:hep-ph/0608337.
- [16] G.P. Lepage, S.J. Brodsky, *Phys. Rev. D* **22** (1980) 2157.
- [17] M. Hoferichter, B. Kubis, J. Ruiz de Elvira, H.-W. Hammer, U.-G. Meißner, *Eur. Phys. J. A* **52** (2016) 331, arXiv:1609.06722 [hep-ph].
- [18] M. Hoferichter, J. Ruiz de Elvira, B. Kubis, U.-G. Meißner, *Phys. Rep.* **625** (2016) 1, arXiv:1510.06039 [hep-ph].
- [19] Y.-H. Lin, H.-W. Hammer, U.-G. Meißner, *Eur. Phys. J. A* **57** (2021) 255, arXiv:2106.06357 [hep-ph].
- [20] H.-W. Hammer, U.-G. Meißner, *Sci. Bull.* **65** (2020) 257, arXiv:1912.03881 [hep-ph].
- [21] Y.-H. Lin, H.-W. Hammer, U.-G. Meißner, *Phys. Rev. Lett.* **128** (2022) 052002, arXiv:2109.12961 [hep-ph].
- [22] J.C. Bernauer, et al., *A1, Phys. Rev. C* **90** (2014) 015206, arXiv:1307.6227 [nucl-ex].
- [23] W. Xiong, et al., *Nature* **575** (2019) 147.
- [24] M. Ablikim, et al., BESIII, *Phys. Lett. B* **817** (2021) 136328, arXiv:2102.10337 [hep-ex].
- [25] M. Ablikim, et al., BESIII, arXiv:2103.12486 [hep-ex], 2021.
- [26] J.P. Lees, et al., BaBar, *Phys. Rev. D* **87** (2013) 092005, arXiv:1302.0055 [hep-ex].
- [27] A. Gasparian, et al., PRad, arXiv:2009.10510 [nucl-ex], 2020.
- [28] T.J. Hague, et al., *Eur. Phys. J. A* **57** (2021) 199, arXiv:2102.11449 [nucl-ex].
- [29] I.T. Lorenz, U.-G. Meißner, H.-W. Hammer, Y.-B. Dong, *Phys. Rev. D* **91** (2015) 014023, arXiv:1411.1704 [hep-ph].
- [30] C. de Calan, H. Navelet, J. Picard, *Nucl. Phys. B* **348** (1991) 47.
- [31] L.C. Maximon, J.A. Tjon, *Phys. Rev. C* **62** (054320) (2000), arXiv:nucl-th/0002058.
- [32] F. Weissbach, K. Hencken, D. Rohe, D. Trautmann, *Phys. Rev. C* **80** (2009) 024602, arXiv:0805.1535 [nucl-th].
- [33] I. Akushevich, H. Gao, A. Ilyichev, M. Mezziane, *Eur. Phys. J. A* **51** (2015) 1.
- [34] A.B. Arbuzov, T.V. Kopylova, *Eur. Phys. J. C* **75** (2015) 603, arXiv:1510.06497 [hep-ph].
- [35] R.D. Bucoveanu, H. Spiesberger, *Eur. Phys. J. A* **55** (2019) 57, arXiv:1811.04970 [hep-ph].
- [36] A. Afanasev, P.G. Blunden, D. Hasell, B.A. Raue, *Prog. Part. Nucl. Phys.* **95** (2017) 245, arXiv:1703.03874 [nucl-ex].
- [37] L.W. Mo, Y.-S. Tsai, *Rev. Mod. Phys.* **41** (1969) 205.
- [38] O. Tomalak, M. Vanderhaeghen, *Eur. Phys. J. A* **51** (2015) 24, arXiv:1408.5330 [hep-ph].
- [39] O. Tomalak, M. Vanderhaeghen, *Phys. Rev. D* **93** (2016) 013023, arXiv:1508.03759 [hep-ph].